Spectral Selective Pencil-Beam Navigator for Abdominal Imaging

M. Köhler[1], C. Moonen[2], and M. Ries[2]
[1]Philips Medical Systems, Finland, [2]IMF, CNRS / Univ. Bordeaux2, Bordeaux, France

Introduction

Recent hardware/methodology developments in the field of MR accelerated the tendency to migrate respiratory gated acquisition schemes for abdominal imaging towards motion compensated strategies such as slice tracking based on pencil-beam navigator data. These permit a continuous acquisition during free-breathing and are thus particularly useful for the continuous guidance of interventional procedures. However, traditional pencil beams have two main disadvantages. Firstly, their presence in the field of view of the imaging sequence causes interference/artefacts and secondly the spin-density-weighted navigator signal suffers from low contrast and consequently poor tracking performance in the abdomen.
As a potential solution to both problems we propose a spectral selective pencil-beam navigator echo. This is achieved by combining three 2D-spatial selective excitation pulses into a 121-binomial pulse sequence which is evaluated theoretically and experimentally in-vivo.

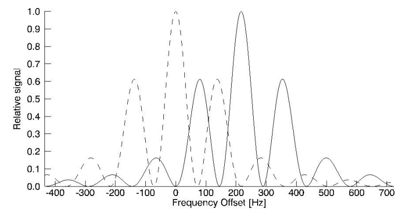

Figure 1. Spectral navigator-selectivity. The solid line in the spectral selectivity graph represents the fat-selective pencil-beam, whereas the dashed line corresponds to the water-selective.

Materials and Methods

The three 2D-spatial selective pulses use a 12-turn spiral k-space encoding as suggested originally by Hardy [1] and in a refined version by Nehrke [2] with a duration of 6.9ms to achieve a water-fat anti-phase condition of $3/2\pi$ after each pulse (flip angle: 25º). Three pulses are used to form a 121-binomial spectral-selective pulse train as suggested by Meyer [3].
The theoretical performance of the pulse was evaluated using the Bloch-simulation software [4] ported to IDL 6.1 (ITT, White Plaines, NY) and extended to employ the 121-binomial pencil-beam navigators. The spatial and temporal resolution of the simulations was 1mm and 6.4µs, respectively, and the simulated FOV 80x80mm^2.
Subsequently, the pulse was implemented on a 1.5T Philips Achieva scanner where the tracking capabilities of the binomial navigator were compared to those of a non-selective navigator on in-vivo kidney. The pencil-beam was placed across the fat capsule of the kidney in head-foot direction. For imaging, a single-shot EPI sequence (TE=30ms, TR=87ms, Resolution=2.3x2.3x6mm^3, Flip=30˚, 121-binomial water sel. pulse) was used.

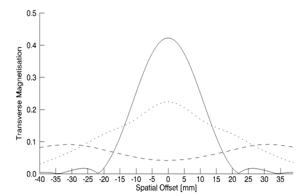

Figure 2. Spatial navigator-selectivity shown through the middle of the beam profile at an offset of 0Hz (solid), 145Hz (dotted) and 290Hz (dashed).

Results and Discussion

Figure 1 shows the simulated spectral selectivity of the proposed navigator pulse, which has a peak-to-valley separation of 72Hz that allows for water selective (resp fat-selective) excitation. Additional spectral peaks occur at 145Hz, 290Hz, 435Hz and 580Hz offset from on-resonance at 1.5T because fat and water will also be in opposite phase at these frequency-offsets. The side-maxima are a consequence of the employed $3/2\pi$ dephasing (compared to the $1/2\pi$ dephasing used in the original 121-binomial pulse train), which is required to provide sufficient time for the spatial encoding.
However, as Figure 2 shows, the spatial selectivity of the pulse is optimal only on-resonance, while quickly falling off for off-resonance signal contributions. The comparison of the magnetization profile perpendicular to the beam direction in Figure 3 depicts the good correspondence between the simulated values and the experimental verification.
Figure 4 shows a comparison of a slice tracking experiment on a human kidney using a spectrally non-selective pencil-beam navigator and the proposed spectral-selective pencil-beam navigator. The spectral-selective navigator shows a good contrast-to-noise ratio and is successful in tracking the organ position over the entire scan duration (2100 images, 3min scanning) without apparent tracking errors. Although the spectrally non-selective navigator shows a higher SNR, the low contrast-to-noise ratio leads to many tracking errors during the scan duration.

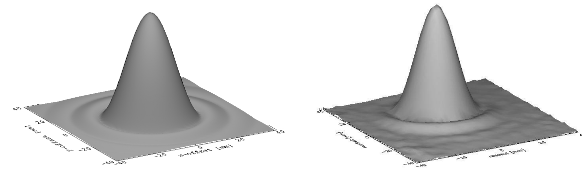

Figure 3. The on-resonance magnetization profile perpendicular to the pencil-beam direction (left: simulation, right: experiment) shows a good spatial localization in the expected form of a Bessel-function.

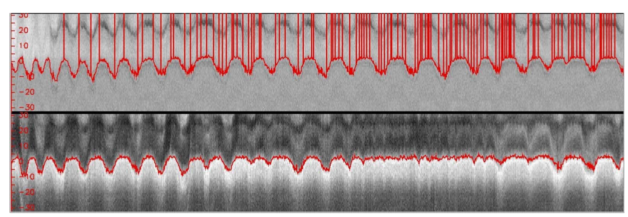

Figure 4. Comparison of the tracking performance on a human kidney under free-breathing conditions between the spectrally non-selective navigator beam (top) and the spectral-selective pencil-beam navigator (bottom) (beam intensity is plotted along the y-axis with increasing dynamic scan numbers to the right, the calculated tracking offset is depicted in red). The non-selective beam suffers from low contrast and thus poor tracking performance, while the spectral-selective beam displays a robust tracking performance through the entire experiment.

Conclusions

Islets of fat-tissue are common around abdominal organs such as the kidney and the liver. Therefore, fat-based navigator echoes can provide positional information derived from high contrast data without interfering with Proton Resonance Frequency (PRF) MR-imaging, even if placed within the field of view of the imaging sequence. The proposed navigator showed an excellent real-time tracking performance for respiratory induced motion compensation for frame-rates of up to 12 images/s. The two main disadvantages are the fairly long encoding time needed to achieve a good resolution in the two spatial and the additional spectral dimension and the requirement of a good shim across the area of interest which should not exceed 1ppm. The proposed navigator is particularly useful for motion compensation of Proton Resonance Frequency-shift (PRFs) based thermometry experiments, since PRF-thermometry commonly discards the fat-signal which is thus available for navigation purposes without interfering with the thermometry.

References

[1] Hardy C.J. et al., J Comput Assist Tomogr, 1991, 15:868-874.
[2] Nehrke K. et al., Magn Reson Imaging, 1999, 17:1173-1181.
[3] Meyer C.H. et al., MRM, 1990, 15:287-304.
[4] http://www-mrsrl.stanford.edu/~brian/bloch/